Performance Evaluation of an Heterogeneous Multi-Robot System for Lunar Crater Exploration

Sebastian Bartsch, Florian Cordes
Stefan Haase, Steffen Planthaber, Thomas M. Roehr

DFKI – Robotics Innovation Center Bremen; 28359 Bremen, Germany
e-mails: firstname.lastname@dfki.de

Abstract

This paper presents the results of the project LUNARES, in which a heterogeneous multi-robot system and a realistic lunar environment replica have been realized in order to evaluate a lunar crater sample return mission. The evaluation shows the general validity and usability of the described approach. The presented experiments include: precision of autonomous docking between heterogeneous robotic systems, parameter selection and energy considerations for climbing a lunar crater with a legged robot, and precision and repeatability of autonomous sample localization and pick up. Critical elements within the mission procedures are identified and improvements to individual components are suggested.

Keywords: Reconfigurable Robots, Heterogeneous Robot Team, Space Robotics, Lunar Crater Exploration, Sample Return

1 Introduction

Space missions so far have been performed with single robots equipped for various mission goals. However, all mobile robotic systems deployed on celestial bodies have in common that they use wheeled locomotion, though in different variations, e.g. recent deployments commonly make use of a rocker-bogie suspension system.

Descending into a (lunar) crater is a challenging task for wheeled robots, and legged locomotion can serve as an alternative solution. A comparison between legged and wheeled motion [7, 9] shows that planar environments are best suitable for wheeled locomotion especially regarding energy efficiency. However, legged systems [10] are able to cope with very rough terrain and slopes, or even climb vertical surfaces [5].

Combining both locomotion principles seems therefore desirable. Huntsberger et al. [4] propose a heterogeneous robotic team for infrastructure/inter-robot servicing and repair. They use a six-legged robot for repairing a rover's wheel. Abad-Manetrola et al. [1] present an ap-
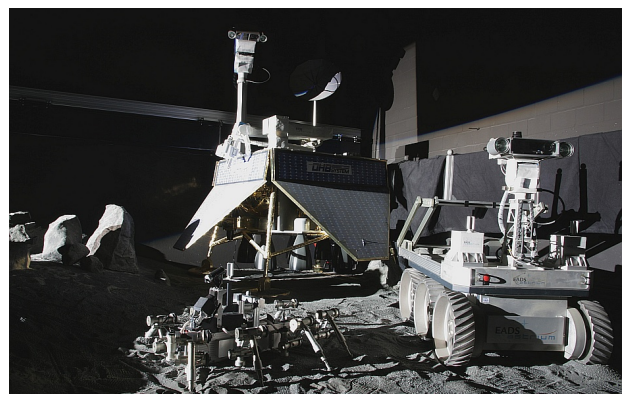
Figure 1. LUNARES systems in artificial crater environment. Left foreground: Legged scout, back in the middle: the landing unit with robotic arm and sensor tower, right foreground: wheeled rover.

proach of using a "classical" rover for longer distances and a scout system for exploration of steep crater environments. The scout system in this approach is a two wheeled system connected via a tether to the main rover.

The project LUNARES evaluates the capabilities of a heterogeneous, reconfigurable robotic team relying on cooperation to fulfil a lunar sample return mission [3]. The project allows a general evaluation of a lunar crater exploration mission, broken down into multiple aspects: cooperation of heterogeneous robotic systems, reconfiguration of robotic systems, control of a mixed human-robot team, and (semi-)autonomous operations in space missions. Furthermore, it shows the usability of a bio-inspired legged robot in space missions [2]. In this paper we will address the following technical issues: (1) autonomously approaching a target sample, (2) collecting the target sample, (3) climbing with a legged robot, and (4) docking of heterogeneous systems.

The anticipated space mission in the project LUNARES is built upon three different robotic systems, Figure 1: a lander, a wheeled rover, and a legged scout.

The current setup assumes that the lander has surfaced the moon, and rover and scout have already disembarked the lander unit. Though the lander has been realized as a scaled down mockup, it provides a robotic arm and a sensor tower. Rover and scout are separate systems, but they can cooperate to form a combined system; the rover can serve as a transport platform for the scout.
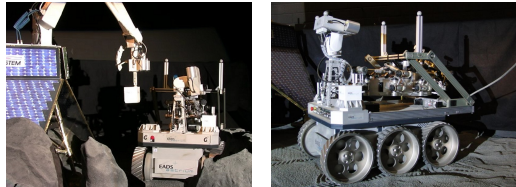
(a) Rover is equipped with a new payload

(b) Rover and scout drive to the crater rim while connected
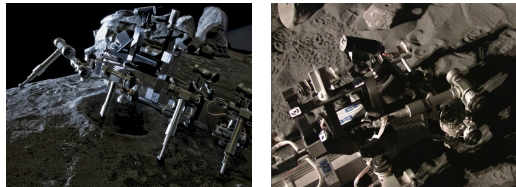
(c) After detaching from the rover, the scout enters the crater

(d) After identifying the sample and successful pick-up, the sample is stowed in the sample container on the scout's back

(e) Scout climbs back up to the rover

(f) Scout docks to the rover, the rover commands the scout

Figure 2. Selected mission steps from the LUNARES demonstration mission.

The mission consists of the following steps (see also Figure 2: After being equipped with a payload (in order to demonstrate the reconfigurability of the system), the rover transports the scout to a crater rim, and unloads the scout. Subsequently, the scout climbs into the crater and requests an operator to select a sample. The scout autonomously approaches the sample and collects it, before carrying it back to the rover. After leaving the crater, the scout docks to the rover for being transported back to the lander. The collected sample is retrieved by the manipulator and stored on the lander where it has to be prepared for its final submission to earth or further analysis. The submission/analysis is not part of the demonstration of the LUNARES project.

2 Autonomous Sample Approach

After reaching the crater bottom, a sample to be picked up is selected by a human operator. The sample is selected by using the camera signal provided by the scout. Using the video image, the scout adapts its position, until the selected sample is in a goal region of the video image. For stability of the approach, the sample is tracked using a particle filter. Due to occlusion the sample can be tracked until it has an approximate distance of 22 cm straight in front of the front right leg of the robot.

2.1 Experimental Setup

The approach has been tested in a dark planar section of the crater bottom. The ground is covered with lunar regolith substitute. The area has not been illuminated directly, except for the robot's infrared lights, which are part of the attached camera, and weak ambient light (which is caused by having a sunlight simulation for the crater rim within a wall-constrained environment).

The approach has been tested for different sample-positions within the robot's coordinate system. The x-axis of the right-handed coordinate system correlates to the forward direction of the robot and the z-axis points upwards.

Because only the approach should be evaluated but not the sample detecting strategy, a retro-reflective ball-shaped marker with a diameter of 21 mm is used as the sample. An single experiment procedure consists of the following steps: (1) operator selects the marker, (2) autonomous approach starts, and (3) autonomous approach ends or is interrupted by the operator. The difference of the reached positions relative to the optimal one - measured within the coordinate system of the robot - are listed in Table 1. The set of experiments covers direct and curved approaches.

For each starting position the sample was approached ten times. The number of manual corrections (reselecting the sample), which were solely necessary due to noisy analog camera transmission[1], has been regarded by the evaluation.

2.2 Experimental Results

The set of experiments and its results are listed in Table 1. The set is designed to reflect the approach under different angles of attack, i.e. approx. 12° and 28° deviation from a straight line. Corrections represents the average number of manual interventions. For our experiments we rely on markers in order to guarantee reproducibility and to avoid influences from the sample detection algorithm. The algorithm does not adapt contrast dynamically but requires an operator to do so.

---

[1]Currently, the processing unit for the camera images remains outside of the actual robot. Thus, analog transmission within the 2.4 GHz band was required to allow image processing.

Table 1. Results of the approach experiments using a reflective marker and a stone as target

| start position x/y cm | Ø duration min:sec | goal position | |
		variance x/y cm	corrections Ø
68 / -31.70	1:05	9.45 / 0.92	0.29
68 / -12.00	1:02	3.61 / 1.57	0.1
48 / -22.40	1:46	5.39 / 1.88	0.3
48 / -8.50	0:52	1.06 / 1.75	0.1
38 / -17.70	0:46	0.73 / 0.18	0.0
38 / -6.70	0:41	0.72 / 1.42	0.0
Ø	1:02	3.49 / 1.29	0.132

2.3 Discussion

The task of approaching the sample has been performed with success and sufficient accuracy. However, the approach showed to be sensitive towards a large distance to the target.

The approach suffered from noisy camera images due to interferences within the wireless network. However, this will not be a problem for robots that have onboard processing capabilites.

The movement of the robot in basalt did not have a major impact on the overall performance. We will show that any inaccuracies of this approach can be compensated by the subsequent steps of sample detection and pick up.

3 Sample Detection and Laser Scanner Evaluation

To start the pickup process of a specific sample, the location of the sample has to be determined accurately. The target sample can be easily determined after generating a height map of the environment and will be further simplified by considering only a region of interest (ROI). This ROI and its size depend on the accuracy of the approach which precedes the sample collect procedure (previous section).

Due to occlusion in the camera image during the autonomous approach, the sample has to be around 22 cm in front of the scouts right "shoulder" (thorax) joint. On this basis the ROI is defined.

Currently a target area of $121\,\text{cm}^2(11\,\text{cm}\times11\,\text{cm})$ applies. The ROI is centered at 22 cm ahead of the thorax joint, which has a static position within the scout's coordinate system.

The scout uses a 3D laser-scanner system to extract a distance image of the environment, which is subsequently transformed into a height map. The essential procedure to extract a sample's position consists of the following steps:

1. Extraction of a laser scan of the direct environment within a horizontal range of ±30°

Table 2. Experimental parameter sets

object type	object size mm	ground material	color grayscale
reflective marker	9	printed paper	161
reflective marker	9	printed paper	127
reflective marker	9	printed paper	69
reflective marker	9	printed paper	0
reflective marker	9	regolith	24-100
reflective marker	19	regolith	24-100
white stone	40	regolith	24-100
white stone	40	regolith	24-100

2. Transformation of the scan data from the scanner coordinate system into the robot coordinate system
3. Generation of the height map in the robot coordinate system
4. Extraction of the region of interest, defining the allowed manipulation area of the scout
5. Extraction of the local extremum within the ROI
6. Extraction of the region around extremum to reconstruct the target center

The height map is transformed into a gray scale image to allow further processing steps such as median filtering.

3.1 Experimental Setup

Repeated tests with the laser scanner have been performed, using the following variables: (1) various sizes of target: spherical with a diameter of 9 mm up to 40 mm, (2) varying types of targets: reflective markers vs. real stone sample, (3) varying grounds: four types of grayscale printed A4 sheets, and regolith covered, and (4) activation of the final software compensation step.

We used a test setup with a table mounted laser scanner, and scanning a sample lying on a fix position. Experiments have been performed in combinations shown in Table 8, where greyscale refer to a printed color sheet.

The regolith used is mainly of darker color, but also contains lighter material resulting in the listed color range from gray scale values of 24 to 100. For each combination 100 scans have been performed. A short warm-up phase of the laser scanner is employed, with five subsequent scans for warm-up. Though this number seems to be small, it proved to be sufficient to create consistent scan results in our scenario.

3.2 Experimental Results

The experiments have shown, that the object detection using the laserscanner is influenced by the color of surface and target object, while the structure of the surface is less important. The grayscale range of 69 to 161 provides a standard deviation of 2 mm up to 5 mm. In contrast a completely black surface causes deviations of 6 mm up to 17 mm depending on the size of the object.

Additionally the deviation increases with the size of the object. Further, the experiment showed a standard de-

viation of about 4 mm for a 19 mm sized sample (20 % of its diameter) versus 14 mm for a 40 mm sized sample (35% of its diameter). However, this deviation is also caused by the fact, that the applied algorithm searches for a pixel with minimum color value within the ROI and thus can be easily affected by measurement noise even after applying a median filter. However, to deal with the measurement noise region growing proofed to be an effective measurement, increasing the accuracy of the sample detection to to standard deviation of 2 mm.

3.3 Discussion

The lunar crater environment creates specific requirements for the approach. The algorithm for autonomous sample detection using laser-scan data has to consider surface and sample color. However, our algorithm would need further evaluation and adaption for inclined or heavily irregular surfaces, since both conditions affect the analysis of the ROI. Nevertheless, we achieved high accuracy after consideration of the environment characteristics and applying region growing to improve the sample center determination. Eventually, this accuracy is sufficient to forward the extracted coordinates to the manipulator leg, which has to deal with play in the joint which is a factor of ten higher than actually needed due to the restricted accuracy of the positioning of the leg (play in the joints).

4 Sample Pickup

To realize the sample collection with the scout a grabbing device has been integrated into the right front leg. The grabber consists of three claws attached to the bottom of the lower leg. One motor is mounted in the shaft of the shank driving the claws through a bevel gear.

After approaching and localizing the sample as described in Section 2 and 3, the grabber has to be moved just above the object in order to collect it. The scout's legs operate with three degrees of freedom. However, due to the kinematics the angle of attack directly depends on the distance to the sample, i.e. the larger the distance to the sample the higher the angle of attack for the grabber (measured from the (vertical) z-axis). The design of the claws has to compensate the kinematic constraint, in order to achieve a high success rate of sample pickups in a wide range of positions. Hence, three different types of claws as illustrated in Figure 3 have been designed and evaluated.

4.1 Experimental Setup

The grabbing process is tested on the bottom of the simulated crater. One out of two different rock samples with a diameter of approx. 45 mm and 30 mm (see Figure 4(a)) is placed at a distance of 170 mm and at
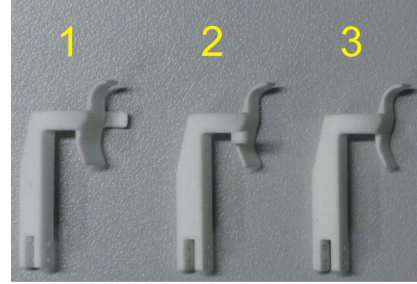
Figure 3. Claw types for scout robot, the claws are with and without a third "finger" at the side.

220 mm from the thorax joint of the right front leg (see Figure 4(b)).

The scout is commanded to collect the sample at the predefined, known position. For each combination of rock samples, claw types and distances ten trials to pick up the sample were performed.
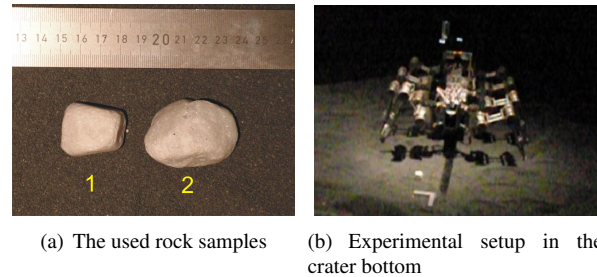
(a) The used rock samples   (b) Experimental setup in the crater bottom

Figure 4. Rock sample and experimental setup

4.2 Experimental Results

The evaluation of the results as presented in Figure 5 shows that the task was performed successfully in 70% over all combinations of experimental paramters with claw type two and three, whereas type one was only successful in 63.5% of the trials. Note that a trial has been counted only as successful if the sample was deposited in the storage unit on the back of the robot. A trial is not successful when (1) grabbing aside of the target, (2) pushing the object away and creating the necessity for a new scan, and (3) loss of the sample while transferring it to the storage unit.

In a more differentiated analysis regarding the rock sample, it can be observed that both the size and shape of the object have a big influence on the success of the collecting process. The smaller sample (1) was collected successfully in 88,33% of all trials but the larger sample (2) only in 46,67%. Claw type two showed most successful trials with sample (1). For sample (2) claw type three was most suitable.
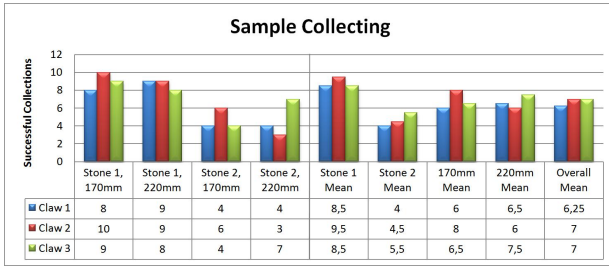
Figure 5. Results of the experimental series

Regarding the different distances in median the sample collection showed a slightly better performance with the smaller distance of 170 mm (68,33%) than with 220 mm (66,67%). This is a slight confirmation of our initial statement, since the angle of attack increases with the distance to the sample.

4.3 Discussion

Due to the fact that the sample gradually leaves the field of view of the camera at a distance smaller than 220 mm this range should not be under-run for the autonomous positioning to the sample described in Section 2. Hence, the third claw type was selected as best suited for the LUNARES mission. With an average success rate of 75% it showed the best performance at this distance. Though the grabbing process can be executed serveral times within the mission, and thus this success rate has a minor impact on the overall mission success.

5 Climbing with Legged Scout Robot

In this experimental series the climbing capabilities of the Scout are evaluated. For locomotion in steep slopes, the original CPG-based locomotion approach [6] has been extended by a state machine containing the four states *stance*, *lift*, *shift* and *touchdown*. The locomotion control allows to set a wide rage of parameters for locomotion of the eight legged robot. In general, the locomotion is cyclic, with the parameter *pulse*, measured in milliseconds. While the allowed time for the three states within the swing phase can be set, the remaining cycle time is used for the stance phase according to Equation 1.

$$t_{stance} = t_{pulse} - (t_{lift} + t_{shift} + t_{touchdown}) \qquad (1)$$

Further parameters include the step width in lateral and transversal direction, and the turning in degrees per cycle. Additionally, body height and body shift can be adjusted. The robot control is also equipped with several reflexes, such as *stumbling correction*, *hole-reflex* for stretching the leg until touching ground to step through small craters, and a *balance-reflex* to shift the center of mass to optimize stability during climbing.

5.1 Experimental Setup

The experimental setup consists of a series of runs in which the scout climbs up the artificial crater slope (distance on optimal path ca. 5 m), guided by an operator. Various locomotion parameters are applied, but are fix for each set of runs. Ten runs with one fix set of locomotion parameters are conducted. The only parameter changing is the heading of the robot, since we need to guide the robot safely to the crater rim.

A power meter installed on the robot is used to evaluate the consumed energy during a single run. Before each run, supply voltage and overall consumed current are recorded. During a run the current and power consumption is recorded for each third of the total distance. After reaching the top of the crater, elapsed time, supply voltage and overall consumed current are recorded. For comparison, similar experiments are conducted on 5 m of flat laboratory floor.

Table 3 lists the walking parameters that were combined in the experimental series. The combination of the parameters results in 12 different parameter sets. Each of the sets is used for at least ten successful runs of the robot in the slope. Since the lean value depends on the slope, a lean value of zero has been used for Scout movements on the laboratory floor. This results in a minimum of 180 runs, since few runs, e.g. due to failed hardware, had to be repeated.

In the following, a pulse value of 3000 (three thousand milliseconds for a full cycle) is noted P3000, the parameter Body Height is abbreviated B150 for a height of 150 mm (distance between center of body and ground). The shift of the body into the slope is denoted as L0, L50 and L100 for zero, 5 cm and 10 cm maximum offset, respectively.

Table 3. Locomotion parameters during climbing experiments

Parameter	Values		
Pulse	3000	4500	
Body Height	150	180	
Max Lean	0	50	100

All experiments were conducted using a phase shift of 0.7. The phase shift denotes the shift between the movement of the single legs of the robot. A phase shift of 1 results in an equally distributed walking pattern, whereas a phase shift of 0 results in a quad-pod-gait, thus four legs are synchronous in stance phase and four legs in swing phase.

5.2 Experimental Results

The experiments showed, that the scout is not able to negotiate the slope at all, when the lean value is restricted

Table 4. Categories of Body Height and maximum Lean value combinations for the conducted experiments

Category	Body Height	Lean Value	Environment
#1	B150	L100	artificial crater
#2	B180	L100	artificial crater
#3	B150	L50	artificial crater
#A	B150	L0	laboratory floor
#B	B180	L0	laboratory floor

Table 5. Average results from runs with P3000 in crater (1-3) and on flat laboratory floor (A,B)

Cat. #	Chrg. mAh	Dev. mAh	Time mm:ss	Dev. mm:ss	Energy Wh	Power W
1	181	26	02:20	00:11	5.62	144
2	262	42	03:28	00:26	8.29	139
3	305	42	03:52	00:29	9.63	151
A	111	6	01:14	00:01	3.49	169
B	132	4	01:16	00:01	4.03	191

to zero (no posture change caused by the inclination). The robot's center of mass (COM) is situated at the lower end of the support polygon, resulting in an increased load on the hind legs, whereas the front legs are hardly supporting traction at all.

With L50 and L100, the robot is able to cope with a slope of approximately 35°. However, using the parameter combination L50, B180 results in heavy slippage and a high risk of tilting over, due to the non-optimal position of the COM. Thus, these experiment series were aborted. Table 4 gives an overview of the combined parameter sets and a category name that is used in the subsequent tables.

Table 5 gives the results of the experiments with P3000, while Table 6 gives the results of the same experiments with P4500. Within one experimental series with the same pulse, the time needed for negotiating the slope represents an indirect measurement of the stability of the locomotion, since heavier slippage results in prolonged climbing to reach the crater rim. This also corresponds with the difficulties, the operator experiences when commanding the robot in the slope. Clearly, the ascend times of the two different series (P3000, P4500) can not be compared to evaluate the stability of the locomotion, since a reduced pulse results in a slower locomotion speed. The average power consumption (W) of the robot is calculated from the measured energy consumption (Wh) and the measured time (s) needed for climbing the slope.

From the data given in the tables it is clearly visible, that the robot's locomotion gets less stable with reduced maximum allowed lean value and increased body height respectively. This can be inferred from the average time needed for ascend as well as in the increased deviation of the run times. This holds for both experimental series (P3000 and P4500). In both series, the stability of

Table 6. Average results from runs with P4500 in crater (1-3) and on flat laboratory floor (A,B)

Cat. #	Chrg. mAh	Dev. mAh	Time mm:ss	Dev. mm:ss	Energy Wh	Power W
1	216	22	03:19	00:10	6.53	118
2	250	29	04:04	00:23	7.80	115
3	342	30	04:59	00:28	10.49	126
A	159	3	02:06	00:02	4.99	143
B	168	20	02:11	00:01	5.28	145

locomotion drops significantly from category #1 (B150, L100) to category #2 and #3, whereas the difference between category #2 and #3 concerning the deviation is not that significant. While the deviation of the ascending time is nearly the same in categories #2 and #3, the overall time needed for ascend is longer when the maximal lean value is restricted (cat. #3) then with increased body height but same max. lean (cat. #2).

Directly dependent on the ascend time is the energy consumption of the robot. This is a general observation, but especially true for legged systems, since in contrast to a wheeled system the robot's actuators have to produce torques constantly, even when the system stands still on even ground. Thus, as expected, the energy consumption increases with the duration of a run.

The comparison of the two series shows another expected result: A slower movement of the robot (P4500) leads to a reduced power consumption. Unexpectedly, the power consumption of category #2 in the slope is less than category #1 for both series. This result cannot be verified in the reference series on even laboratory floor. Here, the expected result of higher power consumption with an higher COM can be observed. Interestingly, the average power consumption in the slope is less than in the reference experiments. The explanation for this observation can be found in the morphology of the scout robot. In thorax and distal joint a high gear ratio is used (higher torques), whereas in the basal joint, a lower gear ratio is used (higher speed). On flat ground, the basal joints have a higher load than in the slope, where a part of the load is transferred to the thorax joints.

For reference, Figure 6 depicts some trajectories of the robot in the slope during the P4500-series. The fastest, slowest and an intermediate run are shown for each parameter category.

5.3 Discussion

As can be seen from the experimental results, a correct parameter choice is crucial for the locomotion of the legged scout in the terrain. Compared to the space of possible parameter sets, the used parameter set for the presented experimental series is relatively small. However, the chosen parameter set shows the whole range of results of different parameters: The results range from not being
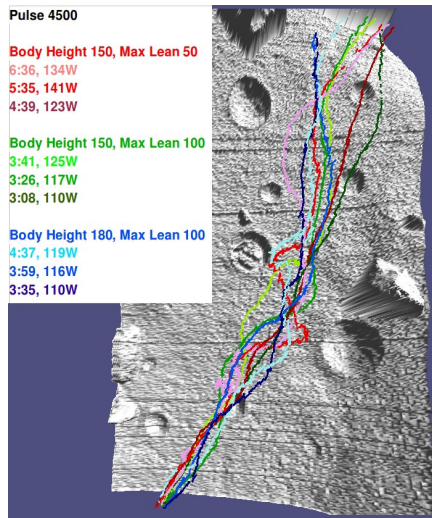
Figure 6. Trajectories of slowest, fastest and intermediate run with P4500 for three parameter sets (B150,L50/ B150,L100/ B180,L100).

able to complete the task at all to success with varying performance concerning energy, power and time needed to ascend in the artificial crater slope.

The mechanical design of the robot also plays an important role in the efficiency for locomotion. The experimental results show, that it is possible to adapt the robot for locomotion in steep slopes by using a specific set of gears in the joints. By optimizing the locomotion for the slope, the efficiency on even terrain might be affected. The reduced gravity on the Moon also has to be taken into account for an actual deployable system.

In general, a trade off between power (W) and energy (Wh) consumption has to be made. For the aspired application of locomotion in a dark crater, the energy consumption plays a greater role, since the robot can not use solar panels for power generation and has to rely on it's batteries completely. Thus, a faster gait should be chosen, since this reduces the energy consumption but yields a higher power consumption.

As a second impact, the reliability of the locomotion has to be taken into account. Clearly, a slower locomotion increases the safety of the locomotion. Dependent on the specific task (how long is the path in darkness, how long is the expected mission duration...) a suitable set of locomotion parameters has to be chosen.

6 Docking

For the LUNARES mission autonomous docking procedures were required for the following situations: (1) The landing unit deploys or extracts a payload from the rover, (2) the scout is transported on the rover. Both docking

procedures are discussed and evaluated in detail in [8]. Hence, and only for completeness, we will present a short summary here.

6.1 Experimental Setup

We evaluated the provided accuracy of the two docking approaches over multiple test sequences using a motion tracking system, which allows tracking with millimeter-precision. The docking of rover to lander, and docking of scout to rover have been evaluated based on ten runs.

Docking Rover to Lander The rover has been placed in various starting positions, though with limited variance due to the constraint of operating in the lunar simulation environment. For the docking process the lander uses a laser scanner to localize the rover based on retro-reflective markers which are attached to the rover. A path is computed from the current rover's position to the target position which the rover follows. When half of the trajectory is completed, a new measurement is done and a new trajectory is generated. This guiding process is repeated until the rover reaches its target position with sufficient accuracy, i.e. it has to be within $0.14\,\mathrm{m}$ of the target position and have an orientation error of less than $2.5°$.

Docking Scout to Rover The scout starts the docking process in various positions and orientations with respect to the rover. The path of the scout is recorded with a motion tracking system. The deviation to the ideal pose of the scout after finishing the docking process is measured.

6.2 Experimental Results

Docking Rover to Lander This docking process showed high accuracies in reaching the final rover target position. The standard deviations are listed in Table 7.

Table 7. Ø-deviations to the target position

x-error	y-error	yaw-error
0.0138 m	0.0098 m	0.36°

Docking Scout to Rover Over the evaluated trials the scout was able to reach the predefined target destination with high accuracy. The given deviations from the target position are listed in Table 8 separately for each degree of freedom. The time for convergence had an average of 184 s with a standard deviation of 35.5 s.

Table 8. Ø-deviations to the target position

x-error	y-error	yaw-error
0.009 m	0.004 m	0.7°

6.3 Discussion

The evaluation performed on the docking procedures in this project has shown, how cooperation of two previously independently operating robots - one being a behaviour-based legged robot - can be achieved by applying visual servoing. The applied control and docking strategy has been robust enough to cope with inaccuracies introduced by the scout. This accuracy allowed to use predefined subsequent mechanical linking procedures.

7 Conclusions and Outlook

In LUNARES we built up an earth demonstrator of a complex robotic mission. The demonstrator is used for evaluation of the heterogeneous robotic approach for retrieval of a sample from within a permanently shadowed crater at the lunar south pole. Preexisting robots have been used for that goal, the robots were not explicitly designed for the chosen mission scenario.

An autonomous approach of the walking scout towards a selected geological sample has been evaluated in this paper. The performance of this rough positioning in front of a promising sample showed to be accurate enough for the following fine detection of the sample's coordinates using a laser scanner. The robustness of the approach was increased using a particle filter for estimation of the sample in the video image.

The fine detection of the sample is done using a laser scanner. A greyscale height map is generated from the laser scan. Using a region growing algorithm the center of the sample is extracted with higher precision than actually needed due to play in the robots joints.

A docking procedure for a walking machine and a wheeled rover was developed. It is based on visual information from the rover's camera system, which is used to control the legged scout. Furthermore, a docking procedure allowing the precise placement of a rover in front of a landing unit was developed using the lander's sensor system. For exchanging payloads and sample containers between rover, scout, and landing unit, visual servoing methods were implemented.

Important experiences with locomotion of walking machines in crater environments were made and the locomotion principle was significantly improved. With appropriate control mechanisms even the Scorpion robot, not explicitly designed for this terrain, was able to climb in the artificial crater with slopes of up to $35°$. The locomotion was safe and reliable, even with leg failure, the robot could negotiate the slope with the remaining seven legs.

The evaluated parts of the mission that are presented in this paper were successfully demonstrated in a complex overall mission. This demonstration showed the ability of the project partners to deal with a complex multi-robot mission and proved the overall system to be capable fetching a soil sample from within a dark crater.

In the project RIMRES[2] (Reconfigurable Integrated Multi-Robot Exploration System [3]) the idea of heterogeneous robotic systems is further pursued. The mobile systems will be newly developed in a co-design process. A standardized mechatronic interface and a connection providing interfaces for exchange of data and energy will be developed, allowing for a closer coupling between rover and scout.

References

[1] ABAD-MANTEROLA, Pablo ; BURDICK, Joel W. ; NESNAS, Issa A. D. ; CHINCHALI, Sandeep ; FULLER, Christine ; ZHOU, Xuecheng: Heterogeneous Robotic Teams for Exploration of Steep Crater Environments. In: *Proceedings of the 2010 IEEE International Conference on Robotics and Automation (ICRA'10)*. Anchorage, Alaska, USA, 2010

[2] CORDES, F. ; PLANTHABER, S. ; AHRNS, I. ; BIRNSCHEIN, T. ; BARTSCH, S. ; KIRCHNER, F.: Cooperating Reconfigurable Robots for Autonomous Planetary Sample Return Missions. In: *ASME/IFToMM International Conference on Reconfigurable Mechanisms and Robots (ReMAR-2009)*. London, United Kingdom, June 22-24 2009

[3] CORDES, Florian ; KIRCHNER, Frank: Heterogeneous Robotic Teams for Exploration of Steep Crater Environments. In: *Planetary Rovers Workshop (ICRA2010)*. Anchorage, Alaska, USA, 2010

[4] HUNTSBERGER, Terry ; RODRIGUEZ, Guillermo ; SCHENKER, Paul S.: Robotics Challenges for Robotic and Human Mars Exploration. In: *Proceedings of ROBOTICS 2000*, 2000, S. 84–90

[5] KENNEDY, B. ; AGHAZARIAN, H. ; CHENG, Y. ; GARRETT, M. ; HUTSBERGER, T. ; MAGNONE, L. ; OKON, A. ; ROBINSON, M.: Limbed Excursion Mechanical Utility Rover: LEMUR II. In: *53rd International Astronautical Congress*, 2002

[6] LINNEMANN, Ralf ; KLAASSEN, Bernhard ; KIRCHNER, Frank: Walking Robot Scorpion - Experiences with a Full Parametric Model. In: KERCKHOFFS, E.J.H. (Hrsg.): *15th European Simulation Multiconference: Modelling and Simulation*. Prague, Czech Republic, June 6-9 2001, S. S.1012–1018

[7] PATEL, Nildeep ; SCOTT, Gregory P. ; ELLERY, Alex: Application of Bekker Theory for Planetary Exploration through Wheeled, Tracked and Legged Vehicle Locomotion. In: *Proc. of Space 2004 Conference*, 2004, S. 1–9

[8] ROEHR, Thomas M. ; CORDES, Florian ; AHRNS, Ingo ; KIRCHNER, Frank: Cooperative Docking Procedures for a Lunar Mission. In: *Proceedings of the ISR/Robotik2010*, 2010

[9] SCHENKER, Paul S. ; HUNTSBERGER, Terry L. ; PIRJANIAN, Paolo ; BAUMGARTNER, Eric T. ; TUNSTEL, Eddie: Planetary Rover Developments Supporting Mars Exploration, Sample Return and Future Human-Robotic Colonization. In: *Autonomous Robots* 14 (2003), Nr. 2-3, S. 103–126

[10] SILVA, Manuel F. ; MACHADO, J.A. T.: A Historical Perspective of Legged Robots. In: *Journal of Vibration and Control* 13 (2007), S. 1447–1486